Available online at www.sciencedirect.com
SCIENCE DIRECT®
Journal of Power Sources 119–121 (2003) 585–590
JOURNAL OF POWER SOURCES
www.elsevier.com/locate/jpowsour

Lithium insertion mechanism in Sb-based electrode materials from ^{121}Sb Mössbauer spectrometry

Laurent Aldon[a], Aurélie Garcia[a], Josette Olivier-Fourcade[a], Jean-Claude Jumas[a,*], Francisco Javier Fernández-Madrigal[b], Pedro Lavela[b], Carlos Pérez Vicente[b], José Luis Tirado[b]

[a]*Laboratoire des Agrégats Moléculaires et Matériaux Inorganiques (UMR 5072 CNRS), Université Montpellier II, CC15 Place Eugène Bataillon, 34095 Montpellier Cedex 5, France*
[b]*Laboratorio de Química Inorgánica, C3 Planta 1, Campus de Rabanales, Universidad de Córdoba, 14071 Córdoba, Spain*

Abstract

Lithium insertion mechanism in some antimony-based compounds: SnSb, $CoSb_3$, $CrSb_2$, $TiSb_2$ has been studied by means of ^{121}Sb Mössbauer spectrometry which gives valuable information about the local electronic structure of the probed element (Sb). The structural and electronic modifications induced by insertion of lithium have been characterized. For these Sb-based materials the lithium insertion mechanisms involve Li_3Sb formation and composite multi-phase separations with one component displaced from the pristine compound.

Keywords: Lithium insertion mechanism; Sb-based materials; ^{121}Sb Mössbauer data

1. Introduction

New interest in the use of lithium–metal alloys as negative materials in lithium-ions batteries has been induced since the announcement of the high performance of tin composite oxides [1]. New materials have been proposed in which the alloying element (like Sn or Sb) is dispersed in an inert matrix [2–5].

Metals (such as Al, Si, Sn, . . .) exhibit large capacities and poor cycling stability due to large volume changes which occur during lithiation/delithiation processes. These effects can be reduced by using intermetallic compounds (alloys) and softened by the existence of multi-phase mechanisms [6–8].

We have studied the effects of electrochemical lithium insertion in Sb metal and some binary compounds such as SnSb, $TiSb_2$, $CrSb_2$, $CoSb_3$ which include p elements (Sn, Sb) and transition elements (Ti, Cr, Co) from ^{121}Sb Mössbauer spectrometry. This hyperfine technique can be used as a probe to investigate changes in the electronic state of the Sb contained within these compounds as a function of the degree of lithiation.

2. Mössbauer spectrometry

Mössbauer spectrometry (recoil-free emission/absorption gamma resonance spectroscopy) is a powerful tool which gives valuable information about the local electronic structure of the probed element (here ^{121}Sb). The hyperfine parameters isomer shift δ (IS) and quadrupole splitting Δ (QS), which are, respectively, linearly dependent on the s-electron density and on the electric field gradient (EFG) at the nucleus, are related to the oxidation states and environments of antimony.

The isomer shift (IS) is measured as the position of the center of gravity of the spectrum relative to that of the appropriate standard reference (InSb). The expression of δ can be written as (1):

$$\delta = S(Z)\frac{Ze^2}{5\varepsilon_0}R^2\frac{\Delta R}{R}\left[|\Psi_a(0)|^2 - |\Psi_s(0)|^2\right] \quad (1)$$

where $\Psi_a(0)$ and $\Psi_s(0)$ are the electron densities at the nucleus of the absorber and source, $R^2\,\Delta R/R$ is the change in the mean-square radius of the nucleus in the Mössbauer transition, $S(Z)$ a term for the relativistic effect, Z is the atomic number, e the charge of the electron and ε_0 is the permittivity of free space. For ^{121}Sb $\Delta R/R < 0$, and any factor which increases the s-electron density (oxidation state, covalency or variations of shielding effect) decreases

* Corresponding author.
E-mail address: jumas@univ-montp2.fr (J.-C. Jumas).

0378-7753/03/$ – see front matter
doi:10.1016/S0378-7753(03)00299-4

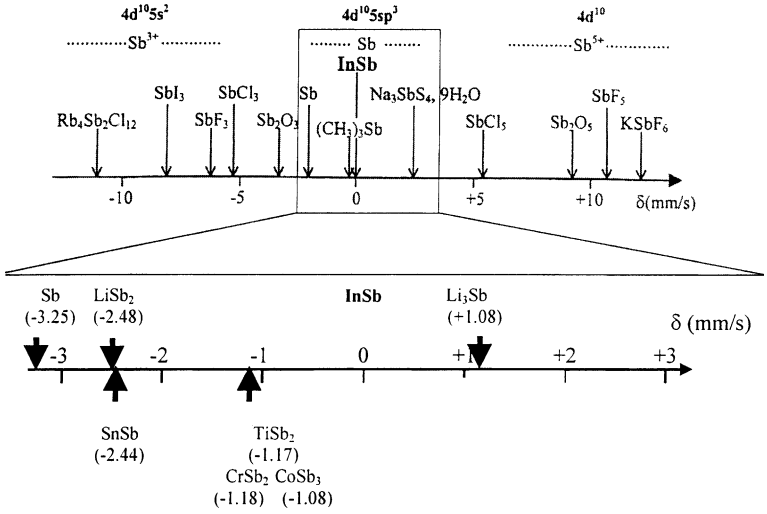

Fig. 1. ^{121}Sb isomer shifts scale from reference compounds [9] and compounds under study.

the IS. The values of IS are qualitatively interpreted with the help of reference compounds [9] (Fig. 1). Quadrupole splitting (QS) arises from the presence of an electric field gradient (EFG) at the Mössbauer nucleus. The expression of Δ is given by Eq. (2):

$$\Delta = \frac{eQV_{ZZ}}{4I(2I-1)}\left[3m_I^2 - I(I+1)\left[1+\frac{\eta^2}{3}\right]\right]^{1/2} \quad (2)$$

where Q is the nuclear quadrupole moment, I the nuclear spin quantum number, m_I the magnetic spin quantum number, V_{ZZ} and η are the EFG and the asymmetry parameter, respectively. The magnitude of QS represents the asymmetry of the electron density around the nucleus and characterizes the arrangements of the probed atom. For ^{121}Sb these two hyperfine parameters (IS and QS) are derived from the analysis of experimental data using transmission-integral procedures [10].

3. Experimental

SnSb, $TiSb_2$, $CrSb_2$ and $CoSb_3$ were synthesized by direct synthesis from the pure elements [4,5] and phase purity was checked by X-ray powder diffraction.

Two-electrode Swagelok cells of the type Li/$LiPF_6$ (mixed organic solvents)/Sb-based materials were used for the electrochemical measurements. Discharges and charges (Fig. 2) were carried under galvanostatic conditions using a Mac Pile II system at $C/4$ rate ($C = 1$ Li (mol $MSb_b)^{-1}$ h^{-1}).

^{121}Sb Mössbauer measurements were performed using a ^{121m}Sn in $BaSnO_3$ source of nominal activity 0.5 mCi on an EG & G constant acceleration spectrometer in transmission mode. During the measurements, both source and absorbers were simultaneously cooled down to 4 K in order to increase the fraction of recoil-free absorption and emission processes. The zero of the isomer shift scale was defined from the spectrum of the reference InSb. Measurements were performed ex situ at several depths of discharge and charge. The Swagelok cells were opened inside a glove box and the electrode materials containing the active material were placed on specific sample holder transparent to the γ rays.

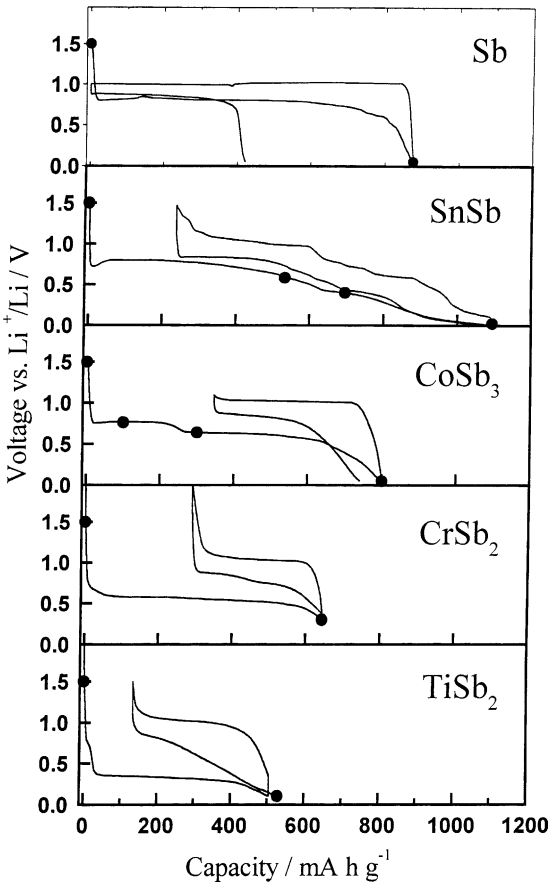

Fig. 2. Charge and discharge curves of some Sb-based compounds. Solid circles indicate the compositions for which ^{121}Sb Mössbauer spectra were recorded.

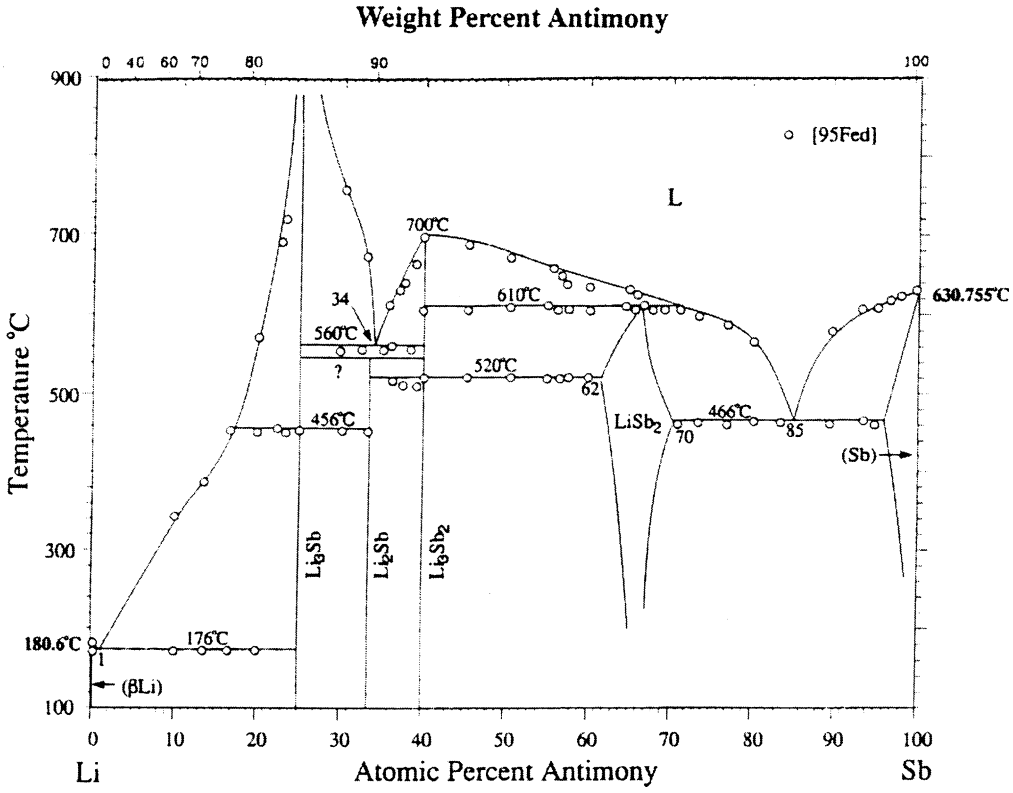

Fig. 3. Li–Sb phase diagram according to [11,12].

4. Results and discussion

The Li–Sb phase diagram [11,12] (Fig. 3) shows the existence of four stoichiometric alloys Li_3Sb, Li_2Sb, Li_3Sb_2 and $LiSb_2$. To our knowledge there are no ^{121}Sb Mössbauer data for these alloys. Nevertheless, ^{121}Sb IS of studied alloys Li_3Sb and $LiSb_2$ in this paper (Table 1) is linearly dependent (Fig. 4) on the atomic ratio Li/Sb. This correlation between IS and composition will be very useful in identifying intermediate compounds during the reaction processes involving lithium and Sb-based materials.

In all cases (Table 1), IS of the studied materials are characteristic of intermetallic compounds (Fig. 1). QS in the range 13–3 mm s^{-1} represent the distortion of the Sb environment. For the pristine compounds, the values of QS are in good agreement with their crystal structure. The linewidth in

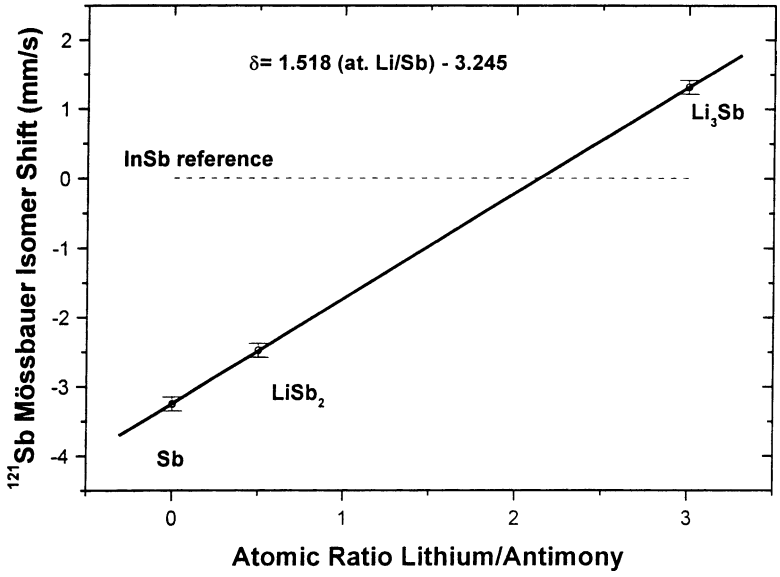

Fig. 4. Linear dependence of the ^{121}Sb Mössbauer isomer shift of Sb, $LiSb_2$ and Li_3Sb vs. Li/Sb atomic ratio.

Table 1
Hyperfine parameters of the refined ^{121}Sb Mössbauer spectra included in Fig. 3

Sample		δ (mm s^{-1})	Δ (mm s^{-1})	Γ (mm s^{-1})	C (%)
References	$LiSb_2$	−2.48 (5)	+4 (1)	1.97 (5)	–
	Li_3Sb	+1.31 (1)	–	1.79 (3)	–
Sb	Pristine	−3.25 (1)	+3.2 (9)	1.79 (9)	–
	0.1 V ≡ $Li_{2.75}Sb$	+1.15 (4)	+7.4 (9)	1.9 (1)	–
SnSb	Pristine	−2.44 (8)	+9 (1)	1.2 (3)	–
	0.6 V ≡ Li_5SnSb	−2.21 (4)	+8.8 (7)	1.0 (1)	–
	0.4 V ≡ Li_6SnSb	−1.99 (4)	+5 (1)	1.8 (2)	–
	0 V ≡ $Li_{10}SnSb$	−2.04 (9)	+5 (2)	1.4 (2)	47
		+0.89 (7)	0	1.4 (2)	53
$CoSb_3$	Pristine	−1.08 (2)	+9.3 (2)	1.61 (4)	–
	0.75 V ≡ $Li_{1.7}CoSb_3$	−1.17 (2)	+9.5 (3)	1.68 (8)	–
	0.6 V ≡ $Li_{4.2}CoSb_3$	−2.4 (2)	+10.9 (8)	1.6 (3)	51
		+1.0 (1)	0	2.8 (2)	49
	0 V ≡ $Li_{10.5}CoSb_3$	+1.08 (1)	0	1.46 (4)	–
$TiSb_2$	Pristine	−1.17 (3)	+10.4 (6)	2.0 (1)	–
	0.1 V ≡ $Li_{5.65}TiSb_2$	−1.6 (2)	+11 (1)	1.5 (2)	60
		+0.8 (2)	0	1.5 (2)	40
$CrSb_2$	Pristine	−1.18 (5)	+16 (1)	4.0 (1)	–
	0.25 V ≡ Li_6CrSb_2	−0.7 (3)	+12.7 (7)	1.29 (8)	45
		+1.29 (5)	0	1.29 (8)	55

δ: isomer shift relative to InSb (−8.70 mm s^{-1} relative to the $Ba^{121m}SnO_3$ source), Δ: quadrupole splitting, Γ: linewidth and C: relative contribution.

the range 1–4 mm s^{-1}, by comparison with the natural linewidth of 2.10 mm s^{-1} for ^{121}Sb, gives informations about site distributions and amorphization. Finally the relative contribution of the different sub-spectra allows to value the proportions of the different Sb species.

The voltage versus composition curves (Fig. 2) show the appearance of different plateaus in the range 0.8–0.5 V. For all materials the first cycle differs from the next ones, showing a large irreversible capacity. X-ray diffraction patterns of the discharged electrodes are characteristic of amorphous compounds [4,5,13] and the use of an alternative technique such as Mössbauer spectrometry is indispensable to complete the characterization. ^{121}Sb Mössbauer spectra obtained at different depths of discharge (marked as solid circles in Fig. 2) are shown in Fig. 5 and the corresponding hyperfine refined parameters are included in Table 1.

At the end of the first discharge, and independently of the nature of the material, the signal of the pristine compound disappears, and a new signal appears, centered at ca. 1–1.3 mm s^{-1} (relative to InSb). The comparison with the IS of pure Li–Sb compounds allows to unequivocally assign this signal to Li_3Sb formation. These results confirm the global reaction (3) based on the simple equation:

$$MSb_b + 3bLi \rightarrow M + bLi_3Sb \quad (3)$$

where $b = 2$ for M = Ti and Cr, and $b = 3$ for M = Co. Nevertheless, in the case of M = Sn (SnSb compound), tin atoms are also involved in the alloying process, yielding a large lithium consumption as previously described in detail [13].

For SnSb and $CoSb_3$ additional samples were prepared at different depths of discharge. The ^{121}Sb Mössbauer spectra are also shown in Fig. 5, and their hyperfine parameters are included in Table 1. In the case of SnSb, a slight shift of the IS is observed, which varies with the lithium content. It indicates that, even if Sb environment is affected during the discharge, its network is somewhat preserved. It suggests that a lithium insertion could take place by occupation of a vacant site or extrusion of tin atom. Fig. 6 summarizes the values of IS as a function of the Li/Sb ratio and shows the existence of two IS ranges, respectively, characteristic of Li–Sb alloys forming (∼1 mm s^{-1}) and $Li_{x+y}M_{1-m}Sb_b$ active matrix (∼0.7 to −2.4 mm s^{-1}). Such an insertion has been previously described in other Sb-based systems, such as InSb [14], where the lithium insertion was accompanied by In extrusion, with changes in the volume cell. Concerning $CoSb_3$, the spectrum at 0.6 V clearly shows the presence of two components. One of them, which appears at ca. 1 mm s^{-1}, can be assigned to Li_3Sb. The other one, at ca. −2.4 mm s^{-1}, is assigned to a modified environment of Sb in $Li_xCo_{1-m}Sb_b$ as compared with the pristine compound $CoSb_3$, and also ascribable to a possible insertion phenomenon. In fact, this insertion was previously suggested in the isoelectronic system $Co_{1-2x}Ni_xFe_xSb_3$ [15].

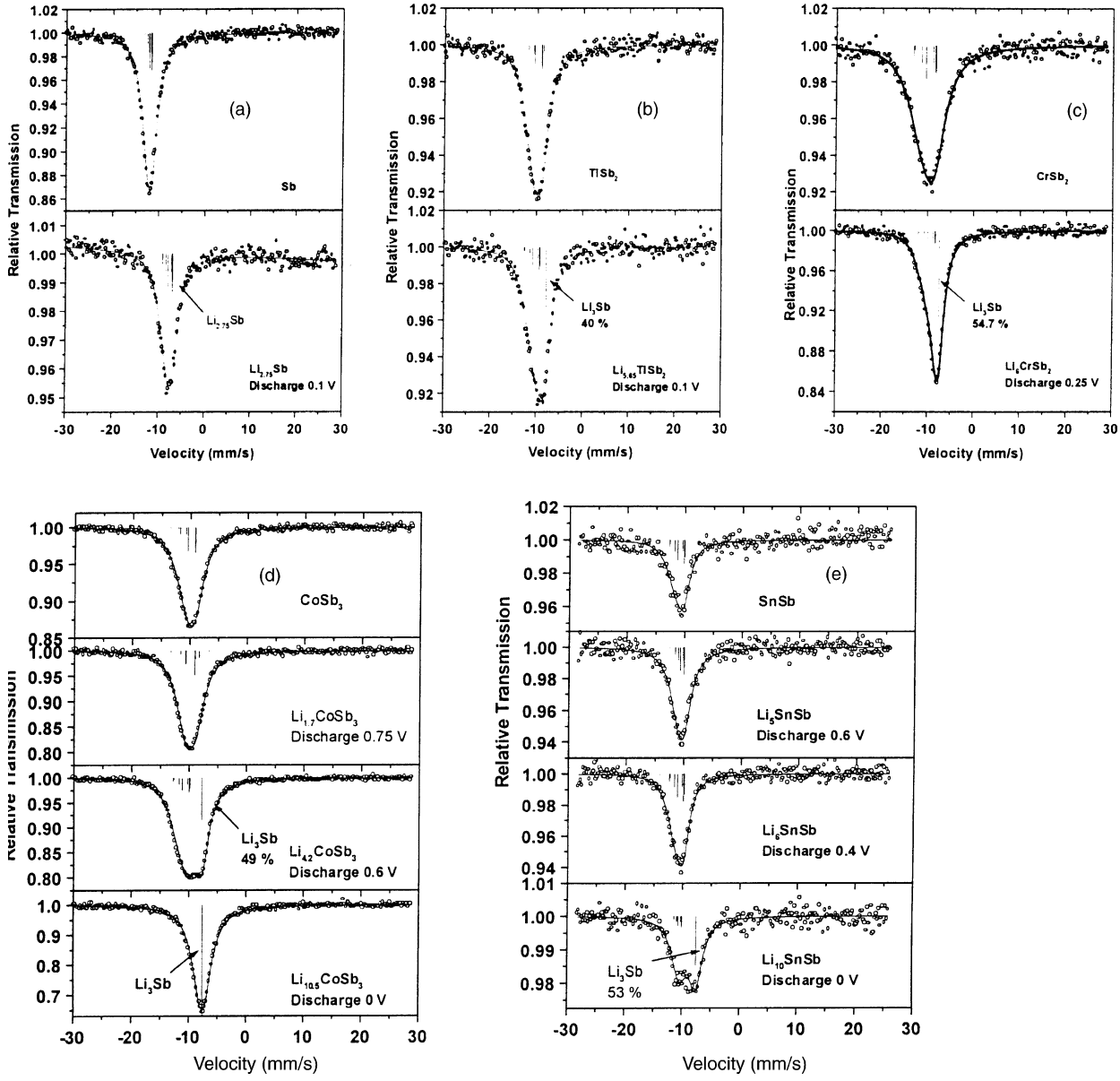

Fig. 5. Changes in the ^{121}Sb Mössbauer spectra of the Sb (a), $TiSb_2$ (b), $CrSb_2$ (c), $CoSb_3$ (d) and SnSb (e) based electrodes during cell discharge, at different nominal compositions.

Taking into account these results, three reactions (4)–(6) can be proposed:

- Lithium insertion in a topotactic reaction (one-phase system, $Li_{1.7}CoSb_3$, Fig. 6):

$$xLi + MSb_b \rightarrow Li_xMSb_b \quad (4)$$

- Lithium insertion with composite multi-phase separation (multi-phase system, Li_5SnSb, Li_6SnSb, $Li_{4.2}CoSb_3$, Fig. 6) with one component displaced from the pristine compound. The ^{121}Sb spectra do not show the presence of metallic Sb. The existence of Li_3Sb in the fully inserted phase is confirmed by the presence in the Mössbauer spectra of a component whose parameters ($\delta \sim 1$ mm s^{-1} and $\Delta = 0$) are close to those of Li_3Sb ($\delta = 1.31$ mm s^{-1} and $\Delta = 0$):

$$Li_xMSb_b + yLi \rightarrow Li_{x+y}M_{1-m}Sb_b + mM \leftrightarrow M + bLi_3Sb \quad (5)$$

Nevertheless, if M is also an active element, as in the case of SnSb, this reaction will be followed by the formation of Li–Sn compounds. The reactions are then:

$$M + ZLi \rightarrow Li_ZM \quad (6)$$

The analysis of the ^{119}Sn Mössbauer spectra of the system Li_xSnSb shows that the presence of metallic tin is clearly proven, as well as the posterior formation of different phases of the Li–Sn system at deeper discharges [13].

Finally, the cycle reversibility takes place between these new phases in a highly dispersed state: active matrix/alloy Li_3Sb for M = Ti, Cr, Co and active matrix/two alloys

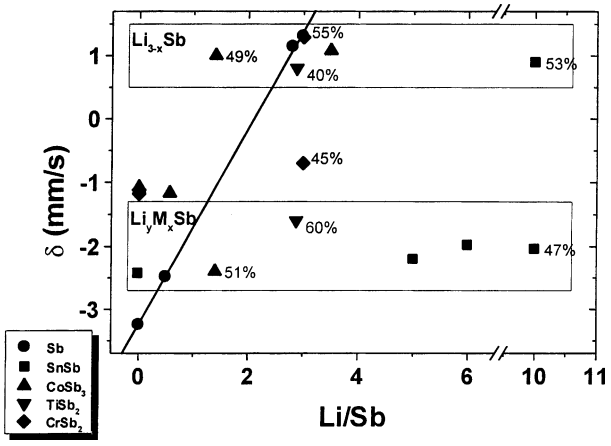

Fig. 6. Correlation between ^{121}Sb IS and the Li/Sb ratio. The percent numbers indicate the relative contributions of the different species.

Li_3Sb, Li_ySn for M = Sn, which illustrate the different mechanisms recently described for anodic materials [6]. At present, additional work is in progress to analyze in detail the evolution and behavior upon cycling.

Acknowledgements

The authors are grateful to CNRS, France (PICS 505), PICASSO, France–Spain Program and CYCIT, Spain (MAT99-0741) for financial support.

References

[1] Y. Idota, T. Kubota, A. Matsufuji, Y. Maekawa, T. Miyasaka, Science 276 (1997) 1395.
[2] J. Chouvin, J. Olivier-Fourcade, J.C. Jumas, B. Simon, Ph. Biensan, F.J. Fernandez-Madrigal, J.L. Tirado, C. Pérez Vicente, J. Electroanal. Chem. 494 (2000) 136.
[3] I.A. Courtney, J.R. Dahn, J. Electrochem. Soc. 144 (1997) 2045.
[4] R. Alcantara, F.J. Fernandez-Madrigal, P. Lavela, J.L. Tirado, J.C. Jumas, J. Olivier-Fourcade, J. Mater. Chem. 9 (1999) 2517.
[5] F.J. Fernandez-Madrigal, P. Lavela, C. Pérez Vicente, J.L. Tirado, J. Electroanal. Chem. 501 (2001) 205.
[6] M. Wachtler, M. Winter, J.O. Besenhard, J. Power Sources 105 (2002) 151.
[7] J.T. Vaughey, C.S. Johnson, A.J. Kropf, R. Benedek, M.M. Thackeray, H. Tostmann, T. Sarakonsri, S. Hackney, L. Fransson, K. Edström, J.O. Thomas, J. Power Sources 97–98 (2001) 194.
[8] H. Li, L. Shi, Q. Wang, L. Chen, X. Huang, Solid State Ionics 148 (2002) 247.
[9] J.G. Stevens, R.M. White Jr., J.L. Gibson, P.C. Newman, D.J. Parker (Eds.), Antimony 121 Handbook: References and Data, Mössbauer Effect Data Center, Asheville, 1985.
[10] K. Rubenbauer, T. Birchall, Hyperfine Interact. 7 (1979) 125.
[11] H. Okamoto, J. Phase Equilib. 17 (3) (1996) 271.
[12] P.I. Fedorov, Russ. J. Inorg. Chem. 40 (5) (1995) 815.
[13] F.J. Fernandez-Madrigal, P. Lavela, C. Pérez Vicente, J.L. Tirado, J.C. Jumas, J. Olivier-Fourcade, Chem. Mater. 14 (2002) 2962.
[14] G. Herren, N.E. Walsöe, Solid State Ionics 47 (1991) 57.
[15] L. Monconduit, J.C. Jumas, R. Alcántara, J.L. Tirado, C. Pérez Vicente, J. Power Sources 107 (2002) 74.